

STAGNET: A SPATIO-TEMPORAL GRAPH AND LSTM FRAMEWORK FOR ACCIDENT ANTICIPATION

Vipooshan Vipulanathan¹, Kumudu Mohottala¹, Kavindu Chinthana¹, Nimsara Paramulla¹, and Charith D. Chitraranjan^{1*}

¹Department of Computer Science and Engineering, University of Moratuwa, Katubedda 10400, Sri Lanka (e-mail: vipooshan.18@cse.mrt.ac.lk, kumudu.20@cse.mrt.ac.lk, kavinduc.20@cse.mrt.ac.lk, nimsara.20@cse.mrt.ac.lk, charithc@cse.mrt.ac.lk)

ABSTRACT

Accident prediction and timely warnings play a key role in improving road safety by reducing the risk of injury to road users and minimizing property damage. Advanced Driver Assistance Systems (ADAS) are designed to support human drivers and are especially useful when they can anticipate potential accidents before they happen. While many existing systems depend on a range of sensors such as LiDAR, radar, and GPS, relying solely on dash-cam video input presents a more challenging but a more cost-effective and easily deployable solution. In this work, we incorporate better spatio-temporal features and aggregate them through a recurrent network to improve upon state-of-the-art graph neural networks for predicting accidents from dash-cam videos. Experiments using three publicly available datasets show that our proposed STAGNet model achieves higher average precision and mean time-to-collision values than previous methods, both when cross-validated on a given dataset and when trained and tested on different datasets.

Keywords Advanced driver assistance systems, Computer vision, Graph neural networks.

1 INTRODUCTION

Accident prediction and timely warnings are vital for improving road safety and minimizing loss of lives and damage to property. Advanced Driver Assistance Systems (ADAS) play a crucial role in supporting human drivers, particularly in anticipating potential accidents before they happen. While many existing systems depend on a range of sensors such as LiDAR, radar, and GPS, relying solely on dashcam video input presents a more cost-effective and easily deployable solution. In this work, we tackle the challenging task of predicting imminent accidents using only dashcam footage. We analyze limitations in current methods and explore strategies to enhance their effectiveness. Our findings highlight significant potential to advance the current state-of-the-art in vision-based accident anticipation systems.

Analyzing dashcam video streams for extracting information for various driver assistance functions is a heavily researched area [1, 2]. In particular, several methods have been proposed to anticipate future accidents. Among them, graph neural network (GNN)-based methods have demonstrated superior performance [3, 4]. However, they do not utilize state-of-the-art techniques to extract spatio-temporal features from video frames containing fast-moving objects. Furthermore, they do not make optimal use of temporal attention. While some methods omit attention mechanisms [3, 5], others use spatial attention only [4]. In recent work, Takur et al. [6] apply temporal attention at the frame-level graph but not at the object-level graph. Furthermore, some of the video datasets widely used to train and test accident anticipation methods suffer from limitations such as video quality bias (e.g., CCD [5], A3D [7]) or a low proportion of ego-involved accidents (e.g., DAD [8]) [3]. However, evaluating these algorithms on unbiased datasets with a large proportion of ego-involved accidents is crucial, as such

incidents are the ones an ADAS can directly mitigate rather than those solely involving other vehicles. Moreover, the generalization of models to datasets beyond those used to train them remains inadequately evaluated due to the use of biased datasets [2].

In this work, we attempt to overcome the aforementioned limitations of existing methods with the following contributions.

- Using more advanced, spatio-temporal features (from SlowFast networks [9]) to represent the input video frames.
- Aggregating frame-level features with a recurrent neural network.
- Applying graph attention to the object-level graph.
- Evaluating the proposed algorithm on unbiased datasets containing ego-involved collisions, including an analysis of its generalization capability across different datasets.

The architectural and feature extraction improvements we propose are simple, yet prove to be highly effective in practice.

2 LITERATURE REVIEW

Typically, accident anticipation methods rely on pretrained convolutional neural networks (CNNs) to detect objects in each video frame and extract features from the detected objects as well as the full frame. We will refer to these as object-level and frame-level features, respectively.

In one of the early works in accident anticipation, Chan et al. [8] proposed a method that feeds the extracted features through a spatial attention mechanism and a recurrent neural network (RNN). This enables the model to learn to focus on important

*correspondence: charithc@cse.mrt.ac.lk

objects based on cues such as their appearance, location, and motion. They have used VGG [10] to extract object-level features. For frame-level features, they have used VGG to extract features from each individual frame and IDT [11] to extract motion-related features from clips of 5 consecutive frames. Suzuki et al. [12] proposed a similar method with the main differences being the use of DeCAF [13] features instead of VGG and a quasi-recurrent neural network [14] for the RNN. Another approach similar to that in [8] was proposed by Karim et al. [15]. They use a similar attention mechanism to weight objects in the same frame (spatial attention). In addition, however, they use a temporal attention scheme where the last M hidden states of the RNN are aggregated as a weighted sum. This allows the model to focus more on important frames in the video.

Several authors have proposed graph neural network-based accident anticipation models. In one of the pioneering works, Bao et al. [5] construct a graph for each video frame such that the nodes represent the objects detected in the frame and edges represent the distance between objects in pixel space. Initial node features are defined as a concatenation of object-level and frame-level features extracted using a pretrained VGG-16 model. The graph is then updated through a graph convolutional network (GCN) and a graph convolutional recurrent network (GCRN) [16] before going through a Bayesian neural network (BNN) [17] to produce the probability of an accident. The BNN also provides the uncertainty associated with the estimated probability. Mahmood et al. [3] proposed a similar graph neural network architecture but noticed that reliance on objects' visual features may hinder the models' ability to generalize to new scenes. To address this, they replaced object-level visual features with geometric features derived from bounding boxes and showed that it improves performance on datasets different from the one used to train the model (cross-dataset evaluation). Thakur et al. [6] proposed a nested graph approach, which further improved the performance. Their work forms the basis for our proposed work and we describe it in more detail in the next section.

In this section, we provided a brief review of the work most relevant to our work. We refer readers to [1, 2] for a more comprehensive review of the literature in accident anticipation.

3 METHODOLOGY

In this work, we propose an improved model to anticipate accidents from dashcam videos based on the Graph(Graph) framework [6]. Given a video consisting of a sequence of observed frames (X_1, X_2, \dots, X_N) , the goal is twofold: (1) to predict whether an accident will occur, and (2) to detect it as early as possible. For each frame X_t , the model outputs a probability p_t indicating the likelihood of an accident occurring in the future. For accident-positive cases, we define the Time-to-Accident (TTA) as $\tau = a - t$ for $t < a$, where a is the start time of the accident and t is the earliest frame such that $p_t > \alpha$, with α being a decision threshold.

The architecture of our model is illustrated in Fig. 1. Similar to the Graph(Graph) model [6], our model consists of three main modules. The first module is responsible for modeling the objects detected in video frames, while the second module extracts the global context of the video frames. The third module

combines the information from the first two modules to provide the final prediction. In the rest of this section, we describe these modules, highlighting the changes we have made with respect to the Graph(Graph) model.

3.1 Spatio-Temporal Object Graph Learning

Not all objects captured by a dash-cam are equally important in assessing collision risk. Typically, objects that are closer to each other and/or closer to the ego-vehicle pose a higher risk of collision. Although it is challenging to accurately measure distances in pixel space with uncalibrated cameras, this module attempts to capture the relationships between traffic objects both within each frame (spatial) as well as across adjacent frames (temporal). The model learns to focus more on relevant objects through the use of spatio-temporal graph attention mechanisms.

We use YOLO [18] to detect objects and extract their bounding boxes from each video frame. For each bounding box, we extract its visual features using a pretrained VGG-16 [10] network, and the word embedding of the objects' class label using GloVe [19]. For a given frame X_t , a spatio-temporal object graph G_t^{obj} with S nodes is constructed, where each node corresponds to a detected object and S is the number of objects detected. The features of each node are initialized with a concatenation of the corresponding objects' visual features $f_e^{\text{obj}} \in \mathbb{R}^{S \times d_1}$ and the word embedding of its class label $f_l^{\text{obj}} \in \mathbb{R}^{S \times d_2}$, where d_1 and d_2 are the visual feature and label embedding dimensions, respectively.

To model intra-frame spatial relationships, a spatial adjacency matrix A_s^{obj} is defined as follows.

$$A_s^{\text{obj}}(i, j) = \frac{e^{-d(c_i, c_j)}}{\sum_{ij} e^{-d(c_i, c_j)}}, \quad (1)$$

where $d(c_i, c_j)$ is the Euclidean distance (in pixel space) between the centers c_i and c_j of the i -th and j -th object bounding boxes detected in a frame, respectively. This ensures that spatially proximate objects contribute more, and distant or irrelevant objects are down-weighted during message passing in the Graph Attention Network that follows.

To model the movement of objects across time, we use a temporal adjacency matrix A_{tm}^{obj} , which links objects of the same class across frames based on the cosine similarity of their features. This temporal graph structure allows the model to propagate information between corresponding objects over time. The temporal adjacency matrix $A_{tm}^{\text{obj}}(i, j)$ is defined as:

$$A_{tm}^{\text{obj}}(i, j) = \begin{cases} s(i, j), & \text{if } l_i = l_j \\ 0, & \text{otherwise} \end{cases}, \quad (2)$$

where $s(i, j)$ is the cosine similarity between the object features of the i -th and j -th objects with labels l_i and l_j , belonging to frames at time t and $t - u$, respectively. These edges ensure the flow of information between the objects of the same class across frames and avoid irrelevant information flow between objects from different classes.

The node embeddings are updated through Graph Attention Networks (GATv2) [20] using the following operations:

$$\begin{aligned}
f_{\text{obj}}^s &= \text{GAT}([\phi(f_e^{\text{obj}}), \phi(f_l^{\text{obj}})], A_s^{\text{obj}}) \\
f_{\text{obj}}^{\text{tm}} &= \text{GAT}([\phi(f_e^{\text{obj}}), \phi(f_l^{\text{obj}})], A_{\text{tm}}^{\text{obj}}) \\
f'_{\text{obj}} &= [f_{\text{obj}}^s, f_{\text{obj}}^{\text{tm}}],
\end{aligned} \tag{3}$$

where ϕ denotes a fully connected layer for dimensionality reduction, and $[\cdot]$ represents concatenation. Note that the original Graph(Graph) architecture used Graph Convolutional Networks (GCN) for this computation. However, we decided to use GATv2 instead as it allows each node in the graph to selectively attend to its neighbors based on its own feature representation and update it accordingly. This graph attention approach, particularly its improved version GATv2, has shown better performance than non-attentive methods such as GCNs on some of the benchmark graph datasets [20]. This attention mechanism can help our model learn to emphasize the most relevant object relationships in the sequence of scenes, improving prediction accuracy and supporting early accident anticipation.

3.2 Spatio-Temporal Global Feature Learning

While the spatio-temporal object graph captures fine-grained object interactions, extracting global contextual features from the entire frame sequence is crucial for providing a holistic understanding of the scene. Most previous approaches [5, 3, 15] rely on pretrained image models such as VGG16 [10] for global feature extraction. However, this does not capture temporal features that span across frames. Thakur et al. [6] extract global frame-level features with I3D [21], which derives features from a sequence of frames, thus capturing both spatial and temporal features. In this work, we utilize a pretrained SlowFast network [9] to extract frame-level spatio-temporal features. SlowFast networks have demonstrated better performance than I3D on video recognition benchmarks and have a dedicated path to process fast movements efficiently. This can be beneficial in processing dash-cam videos, where fast-moving objects are very likely.

To extract the global feature representation f_{fr}^t for a frame at time t , we pass the current frame and the last- u frames $X_{\text{seq}} = (X_{t-u}, \dots, X_t)$ into the SlowFast network, which produces a high-dimensional spatio-temporal representation. These features are then projected into a lower-dimensional space using a fully connected (FC) layer. To further enhance temporal modeling beyond what is captured by the SlowFast network, we pass the transformed features through a Long Short-Term Memory (LSTM) module:

$$\begin{aligned}
f_{\text{fr}} &= \text{SlowFast}(X_{\text{seq}}) \\
f_{\text{fr}}^{\text{fc}} &= \phi(f_{\text{fr}}) \\
f'_{\text{fr}} &= \text{LSTM}(f_{\text{fr}}^{\text{fc}}),
\end{aligned} \tag{4}$$

where ϕ denotes a fully connected layer used for dimensionality reduction. This enriched global representation is subsequently used in the higher-level Spatio-Temporal Global Feature Learning module to support accurate accident anticipation.

3.3 Frame Graph Learning

To capture temporal relationships between video frames, a *frame graph* is constructed that leverages both global frame-level features and object-level features obtained from the previous stage. In this graph, each node corresponds to a frame at a particular time step t , and edges are directed from past frames to the current one, ensuring no future information is leaked backward in time. Each frame node is connected to its previous k frames through k directed edges. The adjacency matrix A_{fr} for the frame graph is defined as:

$$A_{\text{fr}}(i, j) = \begin{cases} 1, & \text{if } i - j \leq k \\ 0, & \text{otherwise} \end{cases}, \tag{5}$$

where i is the index of the current frame node.

Two parallel Graph Attention Network (GAT) layers are applied to this graph. The first GAT layer processes the object-level features f'_{obj} , and the second processes the global frame-level features f'_{fr} :

$$\begin{aligned}
f''_{\text{obj}} &= \text{GAT}(f'_{\text{obj}}, A_{\text{fr}}) \\
f''_{\text{fr}} &= \text{GAT}(f'_{\text{fr}}, A_{\text{fr}}) \\
f'' &= [f''_{\text{obj}}, f''_{\text{fr}}]
\end{aligned} \tag{6}$$

The purpose of applying attention here is to learn which frames are more significant for predicting upcoming accidents. The concatenated feature vector f'' is then passed through fully connected layers to compute the frame-level accident probabilities (p_1, p_2, \dots, p_N) .

The entire model is trained end-to-end, except for the object detection and global feature extraction modules, which are kept frozen. Standard cross-entropy loss is used for optimization:

$$\mathcal{L}(p, y) = - \sum_{m=1}^M y_m \log \left(\frac{e^{p_m}}{\sum_j e^{p_j}} \right), \tag{7}$$

where M is the number of classes (2 in this case), p 's denote the predicted logits, and $y_m = 1$ for the correct ground-truth class label and $y_m = 0$ for all other classes, for a given frame.

4 EXPERIMENTAL EVALUATION

In this section, we detail the experimental setup, including the datasets used, the architecture of the network, the baseline methods for comparison, and the evaluation metrics. We then present and discuss the outcomes of the conducted experiments.

4.1 Experimental Settings

4.1.1 Datasets

We conduct our experiments on three benchmark dashcam video datasets: DAD, DoTA, and DADA. For the Dashcam Accident Dataset (DAD), we use the standard train-test split provided by the Graph(Graph) authors², which is the same as

²<https://github.com/thakurnupur/Graph-Graph>

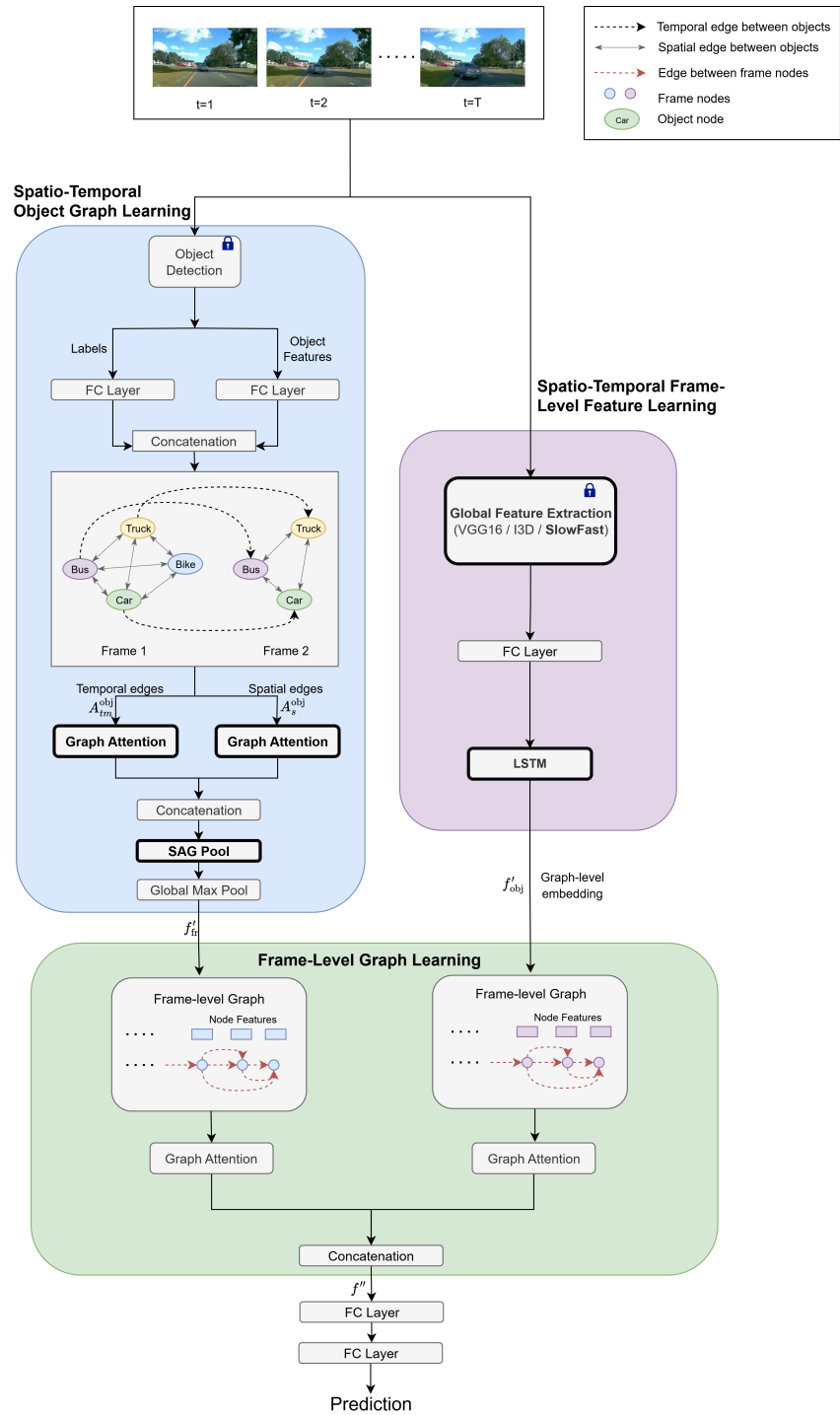


Figure 1: Architecture of the proposed STAGNet accident anticipation framework. Boxes with thicker borders represent the main components introduced in this work.

that used in other works as well, ensuring a fair and consistent comparison with prior work. The DAD dataset comprises 1750 clips extracted from 678 dashcam videos, recorded at 20 frames per second, each lasting 5 seconds. Among these, 620 clips are labeled as accident (positive) and 1130 as normal (negative), with the accident occurring in the last 10 frames of each positive video. Note that this dataset primarily consists of non-ego-involved accidents (less than 10% ego-involved incidents) [15].

Since the anticipation of ego-involved accidents is more important, we evaluate our model on two widely used accident datasets containing a large percentage of ego-involved accidents: DoTA [22] and DADA [23]. We extracted all the ego-involved accidents present in these datasets, which resulted in 745 positive and 745 negative videos from the DoTA dataset, and 965 positive and 1361 negative videos from the DADA dataset. All videos are of 5s duration (similar to DAD). A summary of the characteristics of these datasets is presented in Table 1 and more details can be found in [2]. To eliminate any bias from arbitrary dataset splitting, we adopt a k -fold cross-validation strategy, which allows for a more robust evaluation of model generalization. These datasets provide a diverse set of challenging driving scenarios essential for testing early accident anticipation performance in real-world conditions. To further evaluate model generalization, we conducted cross-dataset evaluation, where the model was trained on DoTA and tested on DADA, and vice-versa. Note that we down-sampled the videos in DADA from 30fps to 10fps for compatibility with those in DoTA to enable direct comparison of results.

Note that we did not include the popular dataset CCD [5] in our evaluation due to its quality bias caused by the difference in video quality between accident and normal videos [3]. This bias can be exploited by models to classify videos based on quality rather than on accident cues. This is evident in the near-perfect performance of all models on CCD.

Table 1: Dataset Statistics.

Dataset	Positive	Negative	Total Videos	FPS
DAD [8]	620	1130	1750	20
DoTA [22]	745	745	1490	10
DADA [23]	938	1361	2299	10

4.1.2 Networks and Baselines

We employ the pretrained object detection model YOLO [18] to extract object-level features. Specifically, we utilize the top 19 detected objects, each represented by a feature vector of dimension $d_1 = 4096$. To encode object labels, we apply GloVe word embeddings [19] using the spaCy library, resulting in embedding vectors of size $d_2 = 300$. Since the video clips are short (5 seconds in length), we set the temporal edge window $u = 1$, meaning each object node is connected only to its counterpart in the previous frame. We fix the number of temporal neighbors at $k = 20$. The architecture and configuration used across all datasets are consistent and illustrated in Fig. 2.

For global visual feature extraction, we adopt the SlowFast network [9], which produces a h -dimensional feature vector for each frame, where $h = 2304$. All experiments are implemented using the PyTorch framework.

On the DAD dataset, we compare our approach against several accident anticipation methods: DSA [8], adaLEA [12], UString

[5], DSTA [15], EGSTL [3], and Graph(Graph) [6]. These algorithms were selected based on their high relevance to this research and widespread use as comparison methods in similar work. The results for these comparative methods are directly taken from the respective publications. We used the same training/testing splits of DAD used by others to obtain the results for our proposed STAGNet model.

On the DoTA and DADA datasets, we compared our model against UString [5], UString (Geometric), and Graph(Graph) [6]. We were unable to compare with the rest of the methods as their implementations were not available for us to run them on DoTA and DADA datasets. Note that we implemented UString (Geometric), as an attempt to mimic GSTL [3], by replacing VGG-based object-level features of UString [5] with geometric features of the detected bounding boxes. Furthermore, although Mahmood et al. [3] have used a similar number of videos from the DoTA dataset, the subset of accident videos selected is different from what we have selected as we specifically selected ego-involved accidents, and they did not. Therefore, results reported in [3] on DoTA are not comparable to what we have achieved.

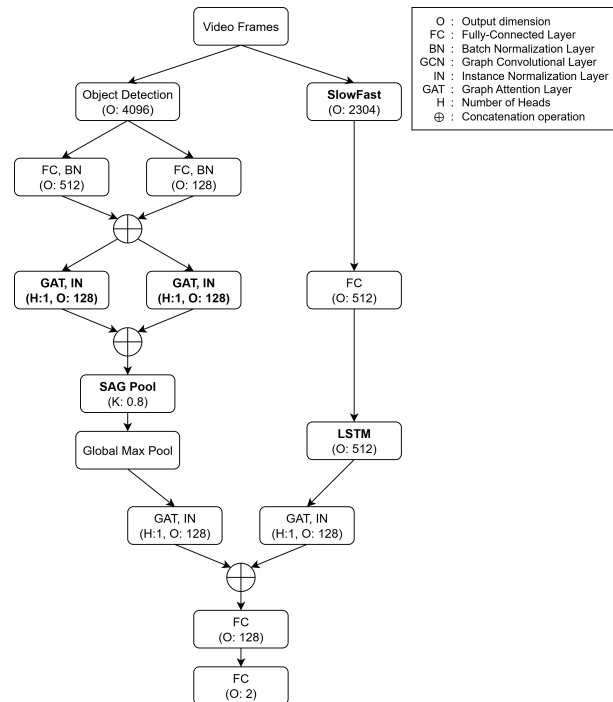


Figure 2: Configuration of the proposed STAGNet accident anticipation framework.

4.1.3 Evaluation Metrics

Accident anticipation models are expected to be both *accurate* and *early* in their predictions. Consistent with prior works [5, 3, 6, 1], we evaluate our model using *Average Precision (AP)* and *mean Time-to-Accident (mTTA)*. AP reflects the correctness of predictions by measuring how well the model distinguishes frames preceding an accident from those with no accident in the near future. For a given frame, if the predicted probability p_i of a future accident exceeds a threshold α , it is counted as a positive prediction. By varying α , a precision-recall curve is

generated, and AP is computed as the area under this curve. A higher AP indicates more accurate predictions.

To determine how early the model can anticipate an accident, we use the *Time-to-Accident (TTA)* metric, which measures the time difference between the actual onset of an accident and the earliest frame, where $p_t > \alpha$. By evaluating TTA across various thresholds α , we compute the *mean TTA (mTTA)* as the average over all corresponding values.

To reduce bias introduced by data splitting, we perform *5-fold cross-validation*, and report the mean of the AP and mTTA values over all folds.

4.2 Results and Discussion

4.2.1 Comparison with State-of-the-art Methods

Table 2 shows the results of the experiments on the DAD dataset. Our proposed algorithm achieves the highest AP and mTTA, closely followed by Graph(Graph) [6]. These two methods perform considerably better than the rest of the comparison methods. The transformer-based method, AAT-ODA [24] achieves very competitive AP but at the expense of a lower mTTA.

Table 2: Performance comparison on DAD Dataset

Dataset	Method	AP (%)	mTTA (s)
DAD [8]	DSA [8]	48.10	1.34
	adaLEA [12]	52.30	3.43
	UString [5]	53.70	3.53
	DSTA [15]	56.1	3.66
	EGSTL [3]	56.30	3.23
	Graph(Graph) [6]	62.80	4.29
	AAT-DA [24]	64.0	2.87
	STAGNet (Ours)	64.36	4.54

As shown in Table 3, for DoTA and DADA datasets with ego-involved accidents, our model clearly outperforms all comparison methods across both datasets. On the DoTA dataset, the UString (Geometrics) and UString models achieve average precisions of 63.16% and 75.40%, respectively, while the Graph(Graph) model reaches 83.50%. In comparison, our model achieves an average precision of 92.73% and an mTTA of 3.23 seconds, meaning the model predicts accidents earlier and more reliably. On the DADA dataset, the performance gap is even more pronounced: our model achieves 95.39% AP, outperforming UString (Geometrics) at 56.75%, UString at 63.95%, and Graph(Graph) at 84.04%. The corresponding mTTA of 3.08s also confirms our methods’ ability to anticipate accidents earlier. These consistent improvements over multiple datasets highlight the effectiveness and robustness of our proposed framework in capturing rich spatio-temporal patterns for early and accurate accident anticipation. In particular, our improved frame-level feature pipeline has a marked effect on predicting ego-involved accidents.

4.2.2 Cross-dataset Evaluation

To assess the generalization capability of our model, we conducted cross-dataset experiments by training on one dataset and evaluating on another. As shown in Table 4, our method consistently outperforms the comparison methods across both datasets. When trained on the DoTA dataset and tested on

Table 3: Performance Comparison of Methods on DoTA and DADA Datasets

Dataset	Method	AP (%)	mTTA (s)
DoTA [22]	UString (Geometrics) [3]	63.16	2.14
	UString [5]	75.40	2.26
	Graph(Graph) [6]	83.50	3.14
	STAGNet (Ours)	92.73	3.23
DADA [23]	UString (Geometrics) [3]	56.75	1.25
	UString [5]	63.95	1.03
	Graph(Graph) [6]	84.04	2.92
	STAGNet(Ours)	95.39	3.08

DADA, our method achieves an AP of 67.47%, outperforming UString (Geometrics) at 46.39%, UString at 48.26%, and Graph(Graph) at 61.34%. Additionally, it achieves a higher mTTA of 3.28s, indicating better anticipation of accidents. Similarly, when trained on DADA and evaluated on DoTA, our method reaches an AP of 80.15%, surpassing UString (Geometrics) at 54.85%, UString at 55.63%, and Graph at 68.55%. It also records a higher mTTA of 3.13s. These results highlight the better generalization ability of our model across datasets.

However, the cross-dataset performance of all tested algorithms is considerably worse than cross-validation results on the same datasets. This can be attributed to the differences in video quality between the two datasets, particularly the higher bit rate [3] in DoTA compared to DADA. The higher bit rate in DoTA results in clearer object boundaries and smoother motion, which can enable the model to learn more detailed spatial-temporal features. However, these learned features may not generalize well to the lower-quality videos in DADA, which contain more compression³ artifacts and reduced detail, thereby degrading cross-dataset performance.

Table 4: Cross-dataset generalization performance on DoTA and DADA. For a given dataset, baseline AP (bAP) = $\frac{\#accident\ videos}{\#all\ videos}$ [25]

Train	Test	Method	AP (%)	mTTA (s)
DoTA [22]	(bAP = 40.8)	UString (Geometrics) [3]	46.39	1.71
		UString [5]	48.26	1.95
		Graph(Graph) [6]	61.34	3.12
		STAGNet (Ours)	67.47	3.28
DADA [23]	(bAP = 50.0)	UString (Geometrics) [3]	54.85	2.45
		UString [5]	55.63	2.17
		Graph(Graph) [6]	68.55	2.86
		STAGNet (Ours)	80.15	3.13

We analyze the impact of various global feature extraction methods on our accident anticipation framework. Since spatial features extracted from pretrained image-based networks such as VGG-16 focus solely on static appearance, they lack the ability to capture temporal dynamics essential for anticipating accidents. To overcome this limitation, spatio-temporal features extracted using I3D and SlowFast networks were explored. As shown in Table 5, the I3D model improves performance over VGG-16 by incorporating motion information across frames. Furthermore, our proposed use of SlowFast yields the best performance, outperforming both VGG16 and I3D. This improvement is attributed to SlowFast’s dual-pathway design, which effectively captures both fast and slow motion cues, providing a richer and more comprehensive spatio-temporal representation.

³<https://github.com/JWFangit/LOTVS-DADA>

These capabilities make SlowFast highly effective for predicting future accidents.

Table 5: Comparison of the effects of different Global Feature Extractors on our STAGNet model

Dataset	Method	AP (%)	mTTA (s)
DoTA [22]	VGG16 [10]	80.89	3.06
	I3D [21]	88.52	2.98
	SlowFast [9]	92.73	3.23
DADA [23]	VGG16 [10]	81.94	2.96
	I3D [21]	89.40	2.92
	SlowFast [9]	95.39	3.08

Table 6: Performance of UString with Global Features extracted from SlowFast network

Dataset	Method	Global Feature	AP (%)	mTTA (s)
DoTA [22]	UString [5]	VGG16 [10]	75.40	2.26
		SlowFast [9]	86.38	1.90
DADA [23]	UString [5]	VGG16 [10]	63.95	1.03
		SlowFast [9]	66.14	1.11

We also evaluated the UString framework by integrating global features extracted from the SlowFast network. The results, as presented in Table 6, show a notable improvement in performance compared to the original UString method, which uses VGG-16 global features. Specifically, the Average AP increased to 86.38 on the DoTA dataset and 66.14 on the DADA dataset, while achieving competitive mTTA values of 1.90s and 1.11s, respectively. This demonstrates that incorporating global context through SlowFast features enhances the anticipation capability of the UString model as well.

4.2.3 Ablation Study

Table 7: Results of the ablation study on the DADA and DoTA datasets. Each model variant removes one or more components (LSTM, GATv2, or SlowFast) to analyze their individual impact. Note: When GATv2 was not used, GCN layers were used. When SlowFast features were not used, I3D features were used.

Data	LSTM	GATv2	SlowFast	Avg AP (%)	Avg mTTA (s)
DoTA [22]	×	×	×	83.50	3.14
	✓	×	×	89.98	3.06
	×	✓	×	85.89	3.13
	×	×	✓	90.03	2.97
	✓	✓	×	88.52	2.98
	✓	×	✓	92.18	3.12
	×	✓	✓	90.75	3.13
	✓	✓	✓	92.73	3.23
DADA [23]	×	×	×	84.04	2.92
	✓	×	×	89.18	2.89
	×	✓	×	84.65	2.96
	×	×	✓	92.95	2.89
	✓	✓	×	89.40	2.92
	✓	×	✓	94.75	3.04
	×	✓	✓	93.51	2.79
	✓	✓	✓	95.39	3.08

The ablation results presented in Table 7 on the DoTA and DADA datasets illustrate the individual contribution of each additional component or modification — LSTM, GATv2, and SlowFast — to the overall performance of our accident anticipation framework.

From the results, it is evident that reverting any of the modifications causes a drop in average precision (AP) on both datasets. However, using SlowFast instead of I3D features and/or adding

an LSTM network in global feature learning has a much larger impact than the addition of GATv2 in object graph learning. For instance, on the DoTA dataset, the baseline without any of the three modifications achieves an AP of 83.50%. Adding the LSTM alone increases AP considerably to 89.98%, indicating the critical role of temporal modeling. Similarly, replacing I3D with SlowFast as the feature extractor itself yields an AP of 90.03%, highlighting the advantage of powerful spatio-temporal feature representations. Combining LSTM and SlowFast further improves performance to 92.18%, and the best results are achieved when all three components (LSTM, GATv2, and SlowFast) are used together, reaching 92.73% AP and an average mTTA of 3.23s. A similar trend is observed on the DADA dataset. The baseline without any modifications yields 84.04% AP, which is improved to 89.18% by adding the LSTM alone. Replacing I3D with SlowFast features as the only modification results in 92.95% AP. Again, the highest performance with 95.39% AP and 3.08s mTTA is attained when all components are used.

The ablation study also reveals that reverting either modification reduces mTTA. Furthermore, we note that neither of the modifications alone improves the mTTA compared to the baseline Graph(Graph) model.

Overall, the ablation study demonstrates that using SlowFast features and/or adding an LSTM module contributes to anticipating accidents much more precisely, while using GATv2 in place of GCN layers in the object graph learning module provides marginal gains. In terms of mTTA, all three modifications are required to anticipate accidents earlier.

4.2.4 Analysis of Execution Speed

Table 8 shows the execution time of different stages in the pipeline for different methods. These experiments were conducted on a computing platform with the following configuration: GPU – Tesla P100 with 16 GiB of memory, CPU – 2-core Intel Xeon (at 2.2 GHz), and 29 GiB of RAM.

According to the results, the most time is taken for detecting objects and extracting VGG-16 features from each bounding box (0.063 s/frame), which is common to all comparison methods. In terms of global feature extraction, VGG is the fastest, followed by I3D and SlowFast, respectively. In terms of model inference time (excluding pre-trained feature extractors), STAGNet and Graph(Graph) operate faster than the BNN-based UString model. Overall, models using VGG-16 or I3D global features operate close to 10 FPS, while our STAGNet model with SlowFast features is slightly slower at 9 FPS. However, we note that the implementations of neither the STAGNet nor other models have been optimized for efficiency. In fact, none of the comparison methods used in this work have previously reported run-times. Therefore, we expect that these models can be made more efficient. Especially, the time-consuming object feature extraction can be parallelized to improve speed.

5 CONCLUSION

In this work, we demonstrate that state-of-the-art graph neural networks for accident anticipation can be substantially improved by using SlowFast networks to extract global, spatio-temporal features of video frames and aggregating them

Table 8: Execution times and speed of different methods. Times for different stages are reported in seconds per frame (s/f), averaged over DoTA and DADA datasets. The overall speed is reported as frames per second (FPS).

Method	Object Detection and Feature Extraction (s/f)	Global Feature Extraction (s/f)	Inference (s/f)	Overall speed (FPS)
UString		0.025 (VGG16)	0.012	9.960
Graph(Graph)	0.063	0.032 (I3D)	0.002	10.199
STAGNet		0.032 (I3D)	0.002	10.197
STAGNet		0.045 (SlowFast)	0.002	9.059

through an LSTM network. Our experiments on benchmark datasets show that the proposed STAGNet model can anticipate ego-involved accidents earlier and more accurately compared to existing methods. Our approach performs better than others even when tested on a dataset different from the one used to train it (cross-dataset evaluation). However, for all algorithms tested, the cross-dataset average precision and mean time-to-accident are notably lower than those achieved when cross-validated on the same dataset. This suggests that further research is needed to investigate and improve the generalization of these models to new environments and traffic conditions.

We note that our model (and other models compared here) is currently not optimized for execution speed. In future work, we will explore techniques to make it more computationally efficient. We also plan to enhance vehicle localization by moving beyond bounding box-based approaches, which can leave empty spaces and fail to tightly encapsulate vehicles, especially along object edges. Utilizing segmentation techniques would allow for more precise delineation of vehicle boundaries, thereby improving detection accuracy. However, this could lead to a reduction in inference speed. Therefore, the trade-offs need to be considered carefully. Additionally, incorporating depth information or utilizing the cameras' intrinsic matrix could enable more accurate estimation of the distance between vehicles, facilitating better scene understanding and potentially improving the robustness of accident prediction models.

REFERENCES

- [1] Jianwu Fang, Jiahuan Qiao, Jianru Xue, and Zhengguo Li. Vision-based traffic accident detection and anticipation: A survey. *IEEE Transactions on Circuits and Systems for Video Technology*, 2023.
- [2] Charith Chitraranjan, Vipooshan Vipulanathan, and Thavarakan Sritharan. Vision-based collision warning systems with deep learning: A systematic review. *Journal of Imaging*, 11(2):64, 2025.
- [3] Farhan Mahmood, Daehyeon Jeong, and Jeha Ryu. A new approach to traffic accident anticipation with geometric features for better generalizability. *IEEE Access*, 11: 29263–29274, 2023.
- [4] Arnav Vaibhav Malawade, Shih-Yuan Yu, Brandon Hsu, Deepan Muthirayan, Pramod P Khargonekar, and Mohammad Abdullah Al Faruque. Spatiotemporal scene-graph embedding for autonomous vehicle collision prediction. *IEEE Internet of Things Journal*, 9(12):9379–9388, 2022.
- [5] Wentao Bao, Qi Yu, and Yu Kong. Uncertainty-based traffic accident anticipation with spatio-temporal relational learning. In *Proceedings of the 28th ACM International Conference on Multimedia*, pages 2682–2690, 2020.
- [6] Nupur Thakur, Prasanth Sai Gouripeddi, and Baoxin Li. Graph (graph): A nested graph-based framework for early accident anticipation. In *Proceedings of the IEEE/CVF Winter Conference on Applications of Computer Vision*, pages 7533–7541, 2024.
- [7] Yu Yao, Mingze Xu, Yuchen Wang, David J Crandall, and Ella M Atkins. Unsupervised traffic accident detection in first-person videos. In *2019 IEEE/RSJ International Conference on Intelligent Robots and Systems (IROS)*, pages 273–280. IEEE, 2019.
- [8] Fu-Hsiang Chan, Yu-Ting Chen, Yu Xiang, and Min Sun. Anticipating accidents in dashcam videos. In *Computer Vision—ACCV 2016: 13th Asian Conference on Computer Vision, Taipei, Taiwan, November 20–24, 2016, Revised Selected Papers, Part IV 13*, pages 136–153. Springer, 2017.
- [9] Christoph Feichtenhofer, Haoqi Fan, Jitendra Malik, and Kaiming He. Slowfast networks for video recognition. *2019 IEEE/CVF International Conference on Computer Vision (ICCV)*, pages 6201–6210, 2018. URL <https://api.semanticscholar.org/CorpusID:54463801>.
- [10] Karen Simonyan and Andrew Zisserman. Very deep convolutional networks for large-scale image recognition. *arXiv preprint arXiv:1409.1556*, 2014.
- [11] Heng Wang and Cordelia Schmid. Action recognition with improved trajectories. In *Proceedings of the IEEE international conference on computer vision*, pages 3551–3558, 2013.
- [12] Tomoyuki Suzuki, Hirokatsu Kataoka, Yoshimitsu Aoki, and Yutaka Satoh. Anticipating traffic accidents with adaptive loss and large-scale incident db. In *Proceedings of the IEEE conference on computer vision and pattern recognition*, pages 3521–3529, 2018.
- [13] Jeff Donahue, Yangqing Jia, Oriol Vinyals, Judy Hoffman, Ning Zhang, Eric Tzeng, and Trevor Darrell. Decaf: A deep convolutional activation feature for generic visual recognition. In *International conference on machine learning*, pages 647–655. PMLR, 2014.
- [14] James Bradbury, Stephen Merity, Caiming Xiong, and Richard Socher. Quasi-recurrent neural networks. *arXiv preprint arXiv:1611.01576*, 2016.
- [15] Muhammad Monjurul Karim, Yu Li, Ruwen Qin, and Zhaozheng Yin. A dynamic spatial-temporal attention network for early anticipation of traffic accidents. *IEEE Transactions on Intelligent Transportation Systems*, 23(7):9590–9600, 2022.
- [16] Youngjoo Seo, Michaël Defferrard, Pierre Vandergheynst, and Xavier Bresson. Structured sequence modeling with graph convolutional recurrent networks. In *Neural Information Processing: 25th International Conference, ICONIP 2018, Siem Reap, Cambodia, December 13–16, 2018, Proceedings, Part I 25*, pages 362–373. Springer, 2018.

- [17] Radford M Neal. *Bayesian learning for neural networks*, volume 118. Springer Science & Business Media, 2012.
- [18] Ao Wang, Hui Chen, Lihao Liu, Kai Chen, Zijia Lin, Jungong Han, and Guiguang Ding. Yolov10: Real-time end-to-end object detection, 2024. URL <https://arxiv.org/abs/2405.14458>.
- [19] Jeffrey Pennington, Richard Socher, and Christopher D Manning. Glove: Global vectors for word representation. In *Proceedings of the 2014 conference on empirical methods in natural language processing (EMNLP)*, pages 1532–1543, 2014.
- [20] Shaked Brody, Uri Alon, and Eran Yahav. How attentive are graph attention networks? *arXiv preprint arXiv:2105.14491*, 2021.
- [21] Joao Carreira and Andrew Zisserman. Quo vadis, action recognition? a new model and the kinetics dataset. In *proceedings of the IEEE Conference on Computer Vision and Pattern Recognition*, pages 6299–6308, 2017.
- [22] Yu Yao, Xizi Wang, Mingze Xu, Zelin Pu, Yuchen Wang, Ella Atkins, and David Crandall. Dota: unsupervised detection of traffic anomaly in driving videos. *IEEE transactions on pattern analysis and machine intelligence*, 2022.
- [23] Jianwu Fang, Dingxin Yan, Jiahuan Qiao, Jianru Xue, He Wang, and Sen Li. Dada-2000: Can driving accident be predicted by driver attention? analyzed by a benchmark. In *2019 IEEE Intelligent Transportation Systems Conference (ITSC)*, pages 4303–4309. IEEE, 2019.
- [24] Yuto Kumamoto, Kento Ohtani, Daiki Suzuki, Minori Yamataka, and Kazuya Takeda. Aat-da: Accident anticipation transformer with driver attention. In *Proceedings of the Winter Conference on Applications of Computer Vision*, pages 1142–1151, 2025.
- [25] Takaya Saito and Marc Rehmsmeier. The precision-recall plot is more informative than the roc plot when evaluating binary classifiers on imbalanced datasets. *PLoS one*, 10(3):e0118432, 2015.